Hyperfine Structure and Octopole Interaction in Stable Bromine Isotopes*

HOWARD HOWLAND BROWN† AND JOHN G. KING
Department of Physics and Research Laboratory of Electronics, Massachusetts Institute of Technology, Cambridge, Massachusetts

(Received 22 July 1965)

The atomic-beam magnetic-resonance method has been used to measure the hyperfine structure of the $^2P_{3/2}$ ground state of Br^{79} and Br^{81}. The values obtained for the nuclear dipole, quadrupole, and octopole constants, uncorrected for second-order perturbations, are in cps:

	Br^{79}	Br^{81}
a	884 811 540±62	953 770 006±62
b	−384 880 292±200	−321 520 344±200
c	163±8	235±8

The positive value of the nuclear dipole moment has been confirmed.

INTRODUCTION

WE have remeasured the hyperfine structure of the $^2P_{3/2}$ ground state of the stable bromine isotopes Br^{79} and Br^{81} by the atomic-beam magnetic resonance method to a precision sufficiently high ($\sim 10^{-7}$) to reveal a previously undetected magnetic octopole interaction. The increased precision relative to the previous experiment was obtained by using a longer transition region and larger beam flux. The new values of the magnetic dipole and electric quadrupole interaction constants confirm the previously obtained values[1] within their uncertainties.

Experiments

The transitions $(3, -1 \leftrightarrow 2, -1)$, $(2, 0 \leftrightarrow 1, 0)$ and $(2, 1 \leftrightarrow 1, 1)$ in both isotopes, which can be identified on the energy-level diagram of Fig. 1, were observed in flop-in[2] by using the Ramsey separated-oscillating-field method[3] at various C magnetic fields from 1.5 G down, the difference between the frequency of the $(2, 1 \leftrightarrow 1, 1)$ and $(2, 0 \leftrightarrow 1, 0)$ lines being used to calibrate the field. The transition $(1, 0 \leftrightarrow 0, 0)$ was observed in flop-out by offsetting the detector from its usual central position. All frequencies were referred to a Cs atomic-frequency standard, and the magnetic field in the C region was investigated both by observing the transitions and by means of a rotating-coil flux meter.

Apparatus

Consult Fig. 2 for quantitative details. The pressure of molecular bromine in the dissociator was controlled by adjusting the temperature of a glass vial containing liquid bromine. Permanent magnet deflecting fields were used. The C field was created by two pairs of coils external to the apparatus so arranged that the earth's field could be bucked out, or any field up to 2 G supplied. The inhomogeneity of the C field, because of the coils, was calculated to be ±0.7%. Transitions were induced by separated fields produced by slanting parallel lines that provided both horizontal and vertical components of the oscillating field. All rf power was generated by klystrons phase-locked to harmonics of a frequency standard controlled by a Hermes crystal oscillator, which was compared with a National 1001 Atomichron. The uncertainty in frequency was less than $\sim 10^{-9}$. A frequency indexer made marks on one channel of a two-channel Sanborn recorder at 60-cps intervals when the frequency of the reference signal generator of the phase lock was swept.

The hot-wire detector was a thoriated tungsten ribbon enclosed with a liquid-N_2 trap in a box to reduce the background arising from contamination of the vacuum envelope by bromine compounds. These compounds had high enough vapor pressure to produce an ion beam in the detector larger than that caused by the

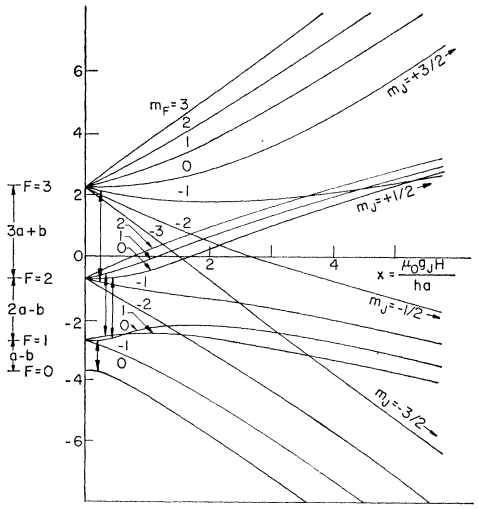

FIG. 1. Energy-level diagram for $I = J = \frac{3}{2}$ and positive nuclear moment (not drawn to scale).

* This work was supported in part by the Joint Services Electronics Program under Contract DA36-039-AMC-03200 (E).

† Present address: Physics Department, New York University, Bronx, New York.

[1] J. G. King and V. Jaccarino, Phys. Rev. **94**, 1610 (1954).

[2] J. R. Zacharias, Phys. Rev. **61**, 270 (1942).

[3] N. F. Ramsey, *Molecular Beams* (Oxford University Press, New York, 1956), p. 124.

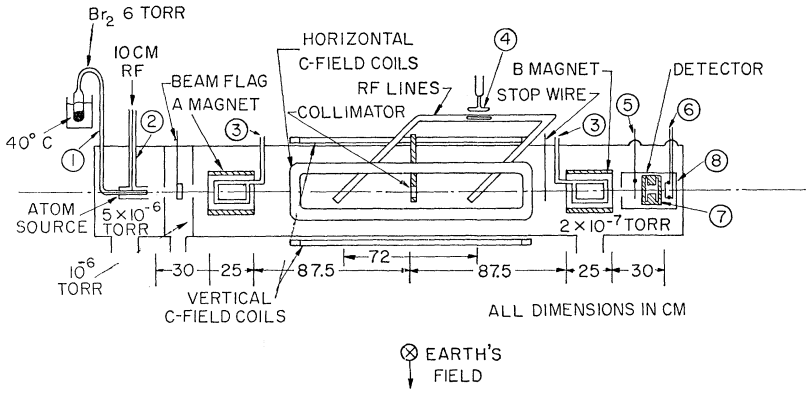

FIG. 2. Side view of apparatus. The atom source[a] consists of an rf discharge in a 7-mm Vycor tube (1) inserted in the drilled-out center of a $\frac{7}{8}$ in. coaxial tee (2). The end of the Vycor tube was sealed off, and a 3-mil slit was cut in it.

The *A* and *B* magnets provided a two-wire field from iron pole pieces of radii: convex 0.250 in., concave 0.312 in. Excitation was supplied by Alnico bars which were usually magnetized by coils (3) to give 3 kg at the beam. The *C* field was produced by two pairs of coils, each pair of coils producing 0.85 G/A at the beam position. Currents were reproducible to less than 5 mA, and the inhomogeneity produced by the coils was calculated to be $\pm0.7\%$. The maximum inhomogeneity in field was ±0.05 G.

The rf lines with which the transitions were induced were made of two 1-in. copper strips separated by $\frac{1}{4}$ in. The entire line was adjustable in length so that it could be made resonant, and was driven by an adjustable coupling loop (4). In practice adjustments were made until the line shape was satisfactory.

The detector consisted of a 0.002×0.010-in. thoriated tungsten ribbon (6) which gives better detection efficiency for bromine than tungsten, but is adversely affected and made unstable by the bromine bombardment. The thoriated ribbon was made sufficiently stable by carburizing[b] it, heating it at 1800°K in 10 Torr of methane for 5 min. The resulting ribbon had a detection efficiency of $\sim10^{-4}$. The noise in the ion beam from the detector was very sensitive to noise in the ribbon heater supply, and large batteries were ultimately used for this purpose.

A mass spectrometer (7) separated the bromine ions from the chlorine ions and electrons emitted by the ribbon. The ion collector (5) was a 40-mil nickel wire. The ion current was measured by a G.E. *FP*-54 electrometer tube in a Dubridge-Brown circuit[c] with a 10^{11} Ω grid resistor and a 5-sec time constant. It was necessary to enclose the entire detector assembly, including the mass spectrometer magnet and ion collector, in a stainless-steel box (8). The box has a directional channel entrance to admit the beam, nichrome heaters, and a liquid-air trap. There is also a door in the box which can be opened and which faces a liquid-air trap. By heating the box, and keeping the liquid-air traps filled, the background was reduced to an acceptable level.

[a] *Advances in Electronics* (Academic Press, Inc., New York, 1956), Vol. VIII, p. 30.
[b] L. R. Koller, *The Physics of Electron Tubes* (McGraw-Hill Book Company, Inc., New York, 1934).
[c] L. A. DuBridge and H. Brown, Rev. Sci. Instr. 4, 532 (1933).

atomic beam. The wire was heated by a power supply that was stable to 10^{-4} to prevent fluctuations in temperature, electron emission, and apparent detection efficiency. The detection efficiency ($\sim10^{-4}$) was estimated by comparing the measured ion current and the magnitude of the atomic beam striking the detector as computed from kinetic theory. In order to maintain maximum detection efficiency it was also found necessary to flash the wire periodically to restore the thorium, and to carburize it with methane to stabilize the work function. A mass spectrometer separated the bromine and chlorine ions emitted by the hot wire. The ion current was measured with an electrometer with a time constant of 5 sec whose output was displayed on the other channel of the two-channel Sanborn Recorder.

DATA

The data taken are listed in Tables I–VI. A correction of ±33 cps (empirically determined) has been applied to take account of the displacement of the resonance peaks caused by the time constant of the electrometer circuit. In Tables I and II the $(2, 1 \leftrightarrow 1, 1)$ and

TABLE I. $(2, 1 \leftrightarrow 1, 1)$ and $(2, 0 \leftrightarrow 1, 0)$ Br^{79} data (all frequencies in cps).

C field current (A)	$(2, 1 \leftrightarrow 1, 1)$	$(2, 0 \leftrightarrow 1, 0)$	0 field interval
+2.348	2154 501 840	2154 495 232	2154 498 775
+2.050	2154 500 934	2154 496 329	2154 498 798
+1.780	2154 500 235	2154 497 175	2154 498 816
−0.683	2154 500 263	2154 497 033	2154 498 765
−0.994	2154 501 105	2154 496 115	2154 498 791
−1.280	2154 502 047	2154 495 033	2154 498 794
		Average =	2154 498 790

TABLE II. $(2, 1 \leftrightarrow 1, 1)$ and $(2, 0 \leftrightarrow 1, 0)$ Br^{81} data (all frequencies in cps).

C field current (A)	$(2, 1 \leftrightarrow 1, 1)$	$(2, 0 \leftrightarrow 1, 0)$	0 field interval
+2.515	2229 057 411	2229 049 575	2229 053 773
+2.326	2229 056 745	2229 050 346	2229 053 774
+2.048	2229 055 912	2229 051 335	2229 053 777
−0.988	2229 056 058	2229 051 081	2229 053 748
−1.286	2229 057 084	2229 049 970	2229 053 782
−1.486	2229 057 831	2229 049 100	2229 053 778
		Average =	2229 053 772

$(2, 0 \leftrightarrow 1, 0)$ frequencies are listed. These frequencies were taken in pairs in magnetic fields large enough to separate the Ramsey patterns. From each pair of frequencies for a fixed magnetic field, the zero-field interval was calculated by using the field dependences in Table VII. Once the zero-field interval was known, either transition was used to calibrate the field for all of the $(1, 0 \leftrightarrow 0, 0)$ data except that of run No. 4. All of the $(1, 0 \leftrightarrow 0, 0)$ data were taken by off-setting the detector, except that of run No. 6, which was obtained by the flop-out on flop-in method.[4]

The $(3, -1 \leftrightarrow 2, -1)$ data, which are in Tables III and IV, were recorded at small values of the C field. The vertical C field was monotonically changed so that the frequencies first decreased and then increased. For small fields, the frequency change is a function of the square of the magnetic field, and hence of the square of the current in the vertical C-field coils. For Br^{81}, the data were plotted directly and a least squares curve drawn, as shown in Fig. 3. For Br^{79}, the frequencies were somewhat more spread out, with none of them near the minimum. Therefore the current I_m in the vertical C-field coils, which made the C field minimum, was subtracted from the currents I that were used to obtain the data, and the resulting number, $(I-I_m)$ squared. A plot of frequency versus $(I-I_m)^2$ is a straight line, the 0 intercept being the minimum frequency (Fig. 4). The minimum frequencies obtained were corrected to zero field by using field dependences in Table VII, and the

TABLE III. $(3, -1 \leftrightarrow 2, -1)$ Br^{79} data (all frequencies in cps).

C field current (A)	Frequency measured
+1.465	2269 555 787
+1.000	2269 555 679
+0.000	2269 555 704
−0.500	2269 555 861
−0.501	2269 555 851
−0.559	2269 555 873

TABLE IV. $(3, -1 \leftrightarrow 2, -1)$ Br^{81} data (all frequencies in cps).

C field current (A)	Frequency measured
+1.456	2539 791 681
+0.986	2539 791 591
+0.699	2539 791 574
+0.378	2539 791 550
+0.000	2539 791 586
−0.467	2539 791 675
+0.378	2539 791 564
+0.700	2539 791 579
+1.020	2539 791 613
+0.000	2539 791 599

[4] L. Davis, Jr., B. T. Feld, C. W. Zabel, and J. R. Zacharias, Phys. Rev. **76**, 1076 (1949).

TABLE V. $(1, 0 \leftrightarrow 0, 0)$ Br^{79} data (all frequencies in cps).

Run No.	Frequency measured	Corrected to 0 field	Calibrating line	Cal. line frequency
1	1269 711 134	1269 701 170	$(2, 0 \leftrightarrow 1, 0)$ Br^{79}	2154 496 045
2	1269 710 354			
	1269 711 404			
	1269 710 408			
	1269 711 458			
Average =	1269 710 905	1269 700 401	$(2, 0 \leftrightarrow 1, 0)$ Br^{79}	2154 495 895
3	1269 711 466			
	1269 711 459			
	1269 711 495			
	1269 711 504			
	1269 711 534			
	1269 711 525			
Average =	1269 711 497	1269 701 131	$(2, 1 \leftrightarrow 1, 1)$ Br^{79}	2154 501 300

TABLE VI. $(1, 0 \leftrightarrow 0, 0)$ Br^{81} data (all frequencies in cps).

Run No.	Frequency measured	Corrected to 0 field	Calibrating line	Cal. line frequency
4	1275 305 618			
	1275 305 024			
	1275 304 898			
	1275 305 197			
	1275 305 054			
	1275 305 024			
	1275 304 988			
	1275 304 724			
	1275 304 958			
	1275 304 964			
	1275 304 658			
	1275 305 444			
Average =	1275 305 046	1275 303 652[a]		
5	1275 314 912			
	1275 314 854			
Average =	1275 314 883	1275 303 669[a]	$(2, 0 \leftrightarrow 1, 0)$ Br^{81}	2229 050 694[a]
6	1275 314 791			
	1275 314 730			
	1275 314 730			
	1275 314 769			
	1275 314 693			
	1275 314 776			
	1275 314 776			
Average =	1275 314 752	1275 303 378	$(2, 0 \leftrightarrow 1, 0)$ Br^{81}	2229 050 650

[a] Magnetic field calculated to be 0.50 G from other data and gaussmeter measurements.

TABLE VII. Second-order field coefficients.

Transition	Coefficients in Mc/sec x^{-2}	Coefficients in cps G^{-2}
Br^{79}		
$(3, -1 \leftrightarrow 2, -1)$	57.94±0.05	257.8±0.3
$(1, 0 \leftrightarrow 0, 0)$	1250.80±0.05	5564.6±0.3
$(2, 1 \leftrightarrow 1, 1)$	298.07±0.05	1326.1±0.3
$(2, 0 \leftrightarrow 1, 0)$	−344.58±0.05	−1533.0±0.3
Br^{81}		
$(3, -1 \leftrightarrow 2, -1)$	41.67±0.05	159.6±0.3
$(1, 0 \leftrightarrow 0, 0)$	1456.81±0.05	5577.7±0.3
$(2, 1 \leftrightarrow 1, 1)$	346.45±0.05	1326.5±0.3
$(2, 0 \leftrightarrow 1, 0)$	−399.86±0.05	−1530.9±0.3

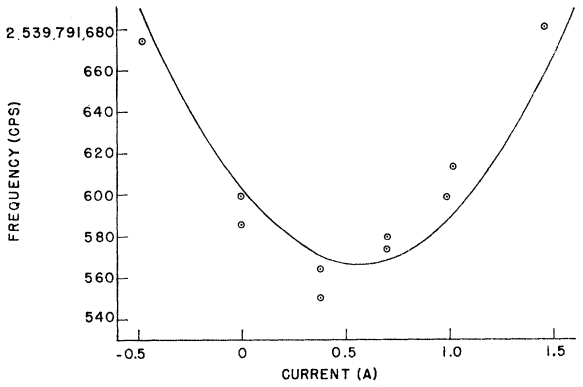

FIG. 3. Frequency of $(3, -1 \leftrightarrow 2, -1)$ resonance in Br^{81} as a function of vertical C-field coil current.

minimum value of the mean-square residual C field, which was determined experimentally to be 0.026 $(G)^2$. The C field was homogeneous to ± 0.05 G. The correction is -4 cps for Br^{81}, and -6 cps for Br^{79}.

Examples of the Ramsey patterns recorded are shown in Figs. 5 and 6. The $(1, 0 \leftrightarrow 0, 0)$ curve differs from the others because the narrower range of atom velocities, which results from displacing the detector, produces many oscillations in the Ramsey pattern, since the interference between atoms of different velocities is reduced. The frequency-marker pips may also be seen in these figures. The average linewidth of the curves, if taken as the difference between the two points where the central peak crosses the base line, was 420 cps.

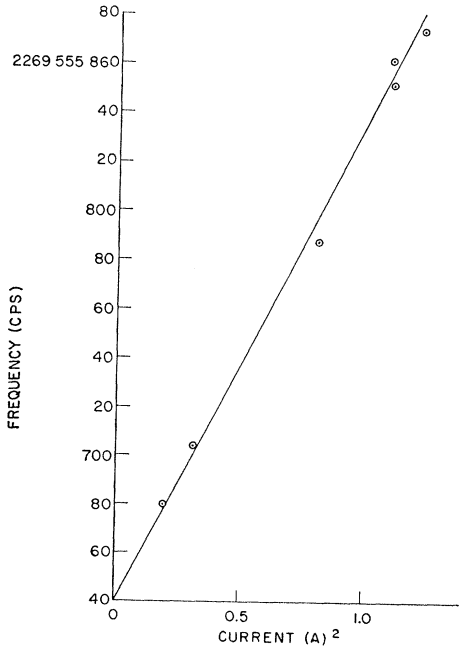

FIG. 4. Frequency of $(3, -1 \leftrightarrow 2, -1)$ resonance in Br^{79} as a function of $(I-I_m)^2$, where I is the current in the vertical C-field coil, and I_m is that current which produces a minimum frequency.

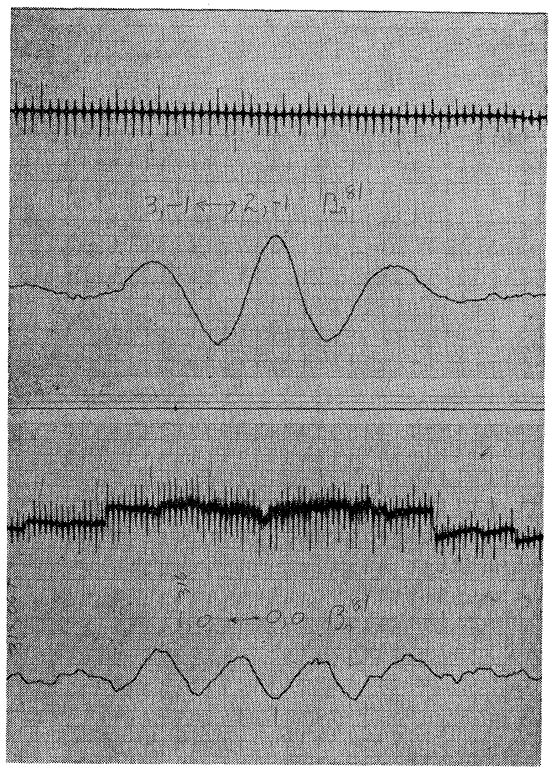

FIG. 5. Representative resonance levels. Top: $(3, -1 \leftrightarrow 2, -1)$ in Br^{81}. Bottom: $(1, 0 \leftrightarrow 0, 0)$ in Br^{81}. Upper trace is frequency indexer $-60\sim$between large spikes.

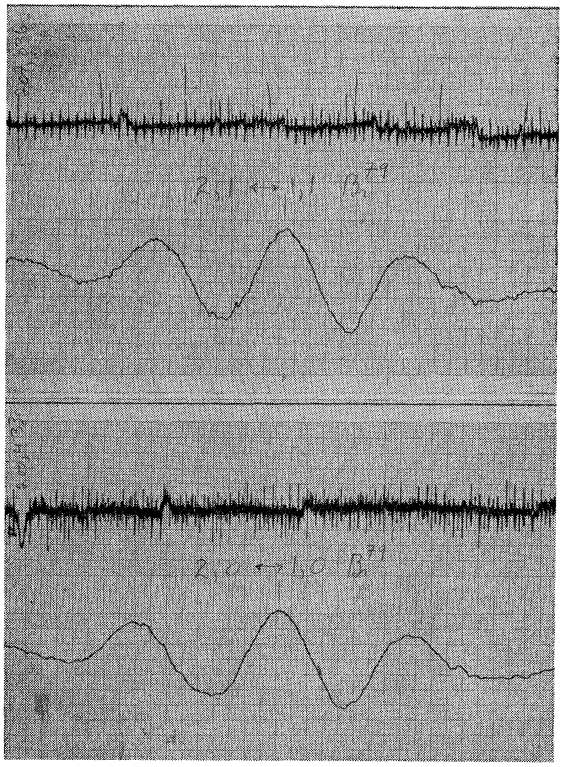

FIG. 6. Representative resonance curves. Top: $(2, 1 \leftrightarrow 1, 1)$ in Br^{79}. Bottom: $(2, 0 \leftrightarrow 1, 0)$ in Br^{79}.

The error in the frequencies measured attributable to the frequency standards, frequency measurements, and the recorder, are estimated to be less than 10 cps. The largest source of error was believed to be possible rf phase differences at the two Ramsey wires.[5] The wires were supposed to be resonant as a whole, which would have guaranteed that the phases at the two transition regions were either in or out of phase, which in turn would have produced symmetrical or antisymmetrical Ramsey patterns. In practice, considerable experimentation had to be carried out both in the length of the transition wires and in the position of the rf feed loop, to obtain reasonably shaped Ramsey patterns. For this reason, the $F=3$ to $F=2$, and $F=2$ to $F=1$ zero-field intervals are assigned uncertainties of ± 100 cps, and the $F=1$ to $F=0$ zero-field intervals are assigned uncertainties of ± 500 cps. The larger error in the latter is due to the poorer signal to-noise ratio, the nature of the Ramsey patterns observed, and the large field dependences of these transitions.

THEORY

The perturbation Hamiltonian expressing the interaction between a point nucleus of spin $I=\frac{3}{2}$, the surrounding electrons with total angular momentum $J=\frac{3}{2}$, and a uniform magnetic field, may be written in the F, m_F representation[6-8] as

$$H_F=\frac{ahK}{2}+\frac{\frac{3}{2}bh[K(K+1)-\frac{4}{3}I(I+1)J(J+1)]}{2I(2I-1)2J(2J-1)}+\frac{(5/4)ch[K^3+4K^2-\frac{4}{5}K[3I(I+1)J(J+1)-I(I+1)-J(J+1)-3]-4I(I+1)J(J+1)]}{I(2I-1)(I-1)J(2J-1)(J-1)}+\mu_0 g_J\mathbf{J}\cdot\mathbf{H}-\mu_n g_I\mathbf{I}\cdot\mathbf{H}, \quad (1)$$

where a, b, and c are the nuclear magnetic dipole, electric quadrupole, and magnetic octopole constants, respectively, $K=F(F+1)-I(I+1)-J(J+1)$, and μ_0 and μ_n are the Bohr and nuclear magnetons, respectively.

For $I=J=\frac{3}{2}$, the first-order transition frequencies in zero magnetic field between successive F levels are

$$X=\frac{W(3)-W(2)}{h}=3a+b+8c, \quad (2a)$$

$$Y=\frac{W(2)-W(1)}{h}=2a-b-28c, \quad (2b)$$

$$Z=\frac{W(1)-W(0)}{h}=a-b+56c. \quad (2c)$$

These three equations can be solved for a, b, and c. The results are

$$a=(1/400)(84X+64Y+20Z), \quad (3a)$$

$$b=(1/400)(+140X-160Y-100Z), \quad (3b)$$

$$c=(1/400)(X-4Y+5Z). \quad (3c)$$

The frequencies are actually measured in a small magnetic field, and are then corrected to zero magnetic field. For small magnetic fields, a perturbation calculation[9] gives the magnetic field dependences of the energy levels $W(F,m_F)$. For $I=J=\frac{3}{2}$, and $c=0$, the frequencies of the transitions, in terms of the dimensionless field parameter $x=\mu_0 g_J H/ah$, are

$$\frac{W(3,m_F)}{h}=\frac{W(3)}{h}+\frac{m_F ax}{2}+\frac{(9-m_F^2)}{20(3a+b)}, \quad (4a)$$

$$\frac{W(2,m_F)}{h}=\frac{W(2)}{h}+\frac{m_F ax}{2}+\left[\frac{(4-m_F^2)}{5(2a-b)}-\frac{(9-m_F^2)}{20(3a+b)}\right]a^2x^2, \quad (4b)$$

$$\frac{W(1,m_F)}{h}=\frac{W(1)}{h}+\frac{m_F ax}{2}+\left[\frac{5(1-m_F^2)}{4(a-b)}-\frac{(4-m_F^2)}{5(2a-b)}\right]a^2x^2, \quad (4c)$$

$$\frac{W(0,0)}{h}=\frac{W(0)}{h}-\frac{5a^2x^2}{4(a-b)}. \quad (4d)$$

The coefficients for x^3 are 0.

In reasonable A and B fields ($x\gtrsim 4$), only the following first-order field-independent transitions will be observable in flop-in: $(3,-1\leftrightarrow 2,-1)$, $(2,1\leftrightarrow 1,1)$, and $(2,0\leftrightarrow 1,0)$. These transitions, plus the $(1,0\leftrightarrow 0,0)$ transition, are the ones that were measured, and are shown in Fig. 1. Their magnetic field dependences have been calculated from Eqs. (4) by using the values of a and b obtained by King and Jaccarino,[1] and the value

[5] *Recent Research in Molecular Beams*, edited by Immanuel Estermann (Academic Press Inc., New York, 1959).
[6] N. F. Ramsey, Ref. 5.
[7] H. B. G. Casimir, *On the Interactions between Atomic Nuclei and Electrons* (Teyler's Tweede Genootschop 11, 36, Haarlem, Netherlands, 1936).
[8] H. B. G. Casimir and G. Karreman, Physica **9**, 494 (1942).
[9] R. L. Christensen, D. R. Hamilton, H. G. Bennewitz, J. B. Reynolds, and H. H. Stroke, Phys. Rev. **122**, 1302 (1961).

of g_J obtained by Harvey, Kamper, and Lea.[10] These field dependences are listed in Table VII.

RESULTS AND CONCLUSIONS

Measured Zero-Field Intervals

The final values given the zero-field $^2P_{3/2}$ hyperfine intervals are as follows (in cps):

Interval	Br^{79}	Br^{81}
$F=1, F=0$	1269 701 000±500	1275 303 515±500
$F=2, F=1$	2154 498 790±100	2229 053 772±100
$F=3, F=2$	2269 555 640±100	2539 791 563±100

Uncorrected Nuclear Constants

The following are the nuclear constants (in cps) uncorrected for any second-order effects:

Constant	Br^{79}	Br^{81}
a	884 811 540±62	953 770 006±62
b	−384 880 292±200	−321 520 344±200
c	163±8	235±8

Sign of the Dipole Moment

The directions of the deflections of the (1,0) and (0,0) states in the A and B magnets depends on the sign of the nuclear dipole moment. By observing which way the detector had to be displaced to observe the $(1, 0 \leftrightarrow 0, 0)$ transitions, the positive moment assigned by King and Jaccarino[1] was confirmed.

Corrected Nuclear Constants

There are two second-order effects on the ground-state hyperfine levels which Schwartz[11–13] has evaluated. The first is the perturbation of the neighboring fine-structure state (for Br, the $^2P_{1/2}$ state), and the second is the effect of configuration interaction of the type in which an outer s electron is raised to a higher s level. With Schwartz' notation, the second-order corrections $W_F^{(2)}$ to the ground-state hyperfine levels of Br^{79} and Br^{81} can be written:

$$W_2^{(2)}=\frac{-1}{144|\Delta E|}\left[-6\eta b-\frac{45}{4}\xi\zeta a\right]^2, \tag{5a}$$

$$W_1^{(2)}=\frac{-20}{|\Delta E|}\left[+\tfrac{1}{4}\eta b-\tfrac{5}{32}\xi\zeta a\right]^2, \tag{5b}$$

$$W_3^{(2)}=W_0^{(2)}=0. \tag{5c}$$

Here, ΔE is the fine-structure splitting, and η and ξ are functions of the normalization constants for the radial wave functions, and of Casimir's relativistic correction factors.[14] For Br, their values are $\eta=1.055$, and $\xi=1.026$.

The factor ζ depends on how much configuration interaction there is, ζ being 1 for no configuration interaction. The evaluation of ζ depends on the ratio $a_{1/2}/a_{3/2}$, where $a_{1/2}$ and $a_{3/2}$ are the nuclear dipole constants of the $^2P_{1/2}$ and $^2P_{3/2}$ ground-state fine-structure levels, respectively. The $^2P_{1/2}$ state has not been measured. We therefore made an empirical estimate of $a_{1/2}/a_{2/2}$, assuming linear relationship between $\beta_{1/2}$ and Z for the s^2p^5 configuration (see Schwartz[15]). This gives a value of 0.008 to $\beta_{1/2}$. Equations (3) and (4) of Schwartz[12] were used to eliminate $a_{1/2}/a_{3/2}$, and to obtain a value of $\beta_{3/2}$. The equation[13]

$$\zeta=1-\beta_{3/2}(1+16/\xi) \tag{6}$$

was then used to evaluate ζ. The result is $\zeta=1.20$. The values of the hyperfine integrals given by Schwartz[13] and corrected for exchange matrix elements, have been used throughout.

By using these values of η, ξ, and ζ, the energy differences X, Y, and Z were corrected, and the nuclear constants computed. The corrected values of a, b, and c are (in cps):

Constant	Br^{79}	Br^{81}
a	884 809 774±62	953 768 180±62
b	−384 882 835±200	−321 524 277±200
c	388±8	430±8

Octopole Moments

Schwartz[13] has calculated the following expression for the nuclear octopole moment Ω in units of nuclear magneton barns (nm b):

$$\Omega=\frac{c\mu F_{3/2}\times 1.96\times 10^8}{a_{3/2}IT(1-\beta_{3/2})Z^2}. \tag{7}$$

$F_{3/2}$ and T are relativistic correction factors. For their

TABLE VIII. Octopole data.

	c_{meas}(cps)	c_{corr}(cps)	Ω (nm b)
Cl^{35}	9.30± 1.2[a]	−6.95± 1.2	−0.0188
Cl^{37}	5.35± 1.2[a]	−5.41± 1.2	−0.0146
Ga^{69}	50.2 ± 3.3[b]	93.0 ± 3.4	0.137
Ga^{71}	86.0 ± 3.3[b]	121.9 ± 3.4	0.180
Br^{79}	163 ± 8[c]	388 ± 8	0.116
Br^{81}	235 ± 8[c]	430 ± 8	0.129
In^{115}	82 ± 32[d]	1682 ± 40	0.475
I^{127}	2870 ±370[e]	2010 ±520	0.181

[a] J. H. Holloway, Ph.D. thesis, Department of Physics, MIT, 1956 (unpublished).
[b] R. T. Daly, Jr. and J. H. Holloway, Phys. Rev. **96**, 539 (1954).
[c] Present work. N. B. No estimate of error in the theoretical correction has been included.
[d] P. Kusch and T. G. Eck, Phys. Rev. **94**, 1799 (1954); C. Schwartz (private communication).
[e] V. Jaccarino, J. King, R. Satten, and H. Stroke, Phys. Rev. **94**, 1798 (1954).

[10] J. S. M. Harvey, R. A. Kamper, and K. R. Lea, Proc. Phys. Soc. (London) **76**, 979 (1960).
[11] C. Schwartz, Phys. Rev. **97**, 380 (1955).
[12] C. Schwartz, Phys. Rev. **99**, 1035 (1955).
[13] C. Schwartz, Phys. Rev. **105**, 173 (1957).
[14] H. Kopferman, *Nuclear Moments* (Academic Press Inc., New York, 1958).
[15] C. Schwartz, Phys. Rev. **105**, 173 (1957), see Fig. 4.

ratio, we used the value 1.236 given by Schwartz. The values of μ were taken from Walchli.[16] The Ω's obtained are: $\Omega(Br^{79})=0.116$ nm b, and $\Omega(Br^{81})=0.129$ nm b. Schwartz points out that there may be significant polarization corrections to Eq. (7).

The octopole moments above may be compared with the single-particle octopole moments calculated by Schwartz.[11] These are $\Omega(l+\frac{1}{2})=0.262$ nm b, $\Omega(l-\frac{1}{2})=-0.0106$ nm b. It is seen that the experimentally obtained values lie well between these limits. We include in Table VIII a previously published table[17] with the values of the c's and Ω's for bromine included.

[16] H. F. Walchli, U. S. Atomic Energy Commission Report ORNL-1469, 1953 (unpublished).
[17] C. Schwartz, Phys. Rev. **105**, 180 (1957); see Table III.

Ratios of the Interaction Constants

Our ratio of a^{81}/a^{79} is 1.0779358(2). This agrees within experimental error with the ratio of the dipole moments obtained by Walchli[16] by nuclear magnetic resonance, which was $\mu^{81}/\mu^{79}=1.07796(2)$. Our ratio of b^{79}/b^{81} is 1.1970568(15), which agrees within the error assignments with the ratio of the quadrupole moments obtained by Schawlow[18] using quadrupole resonance, which was $(eqQ)^{79}/(eqQ)^{81}=1.19707(3)$.

ACKNOWLEDGMENTS

The authors wish to thank Professor C. L. Searle, Dr. R. F. C. Vessot, and Dr. Rainer Weiss for assistance and many fruitful suggestions. The continued help and interest of Dr. J. R. Zacharias has been gratefully appreciated.

[18] A. L. Schawlow, J. Chem. Phys. **22**, 1211 (1954).

PHYSICAL REVIEW VOLUME 142, NUMBER 1 FEBRUARY 1966

Auto-Ionizing States in Helium*

LESTER LIPSKY† AND ARNOLD RUSSEK
Department of Physics, The University of Connecticut, Storrs, Connecticut
(Received 20 June 1965; revised manuscript received 8 October 1965)

The validity of the method of diagonalizing a truncated, finite-dimensional submatrix of the Hamiltonian for the calculation of some properties of some autoionizing states is demonstrated, using projection operators. The truncation procedure is shown to be an example of the Feshbach formalism. It differs from other approaches employing the Feshbach formalism mainly in point of view and in the particular choice of the projection operators. Detailed calculations using the diagonalization method are carried out for the lowest autoionizing states of helium with symmetry $^1S^e$, $^1P^o$, or $^3P^o$. The basis used for the singlet S states is of dimension 42, including all properly antisymmetrized hydrogenic functions with $Z=2$ for all angular configurations up to g-g. For the P states all angular configurations up to f-g are included, resulting in a 55-dimensional basis set. The eigenvalues are compared in detail with several different calculations of resonances in e-He^+ elastic scattering, and with the observation of these states by optical absorption in He and by inelastic scattering of electrons, protons and H_2^+ on He. The eigenvectors are considered to represent the doubly excited states after the excitation has occurred and before they decay, so that they can be used to calculate absorption cross sections and lifetimes. The detailed characteristics of the eigenvectors corroborate the classification scheme of Cooper, Fano, and Prats as far as they have gone. Good agreement is also found between the calculated level structure and the experimental results.

I. INTRODUCTION

ONE of the main objectives of the present work is the calculation of auto-ionizing energy levels in helium. These energy levels have a clear and definite existence experimentally. They show up as sharp maxima in optical-absorption experiments and as resonant peaks of the cross section in electron-scattering experiments.[2] These levels can also be inferred from the distribution-in-energy of the ejected electrons in ion-atom collisions.[3] In molecular physics, such states are required to account for resonant charge-exchange phenomena in He^+-He collisions.[4]

If resonances resulting from collision processes which are fundamentally different in nature (e.g., e^- on He^+, e^- on He, $h\nu$ on He, He^+ on He, H_2^+ on He, He on He) have any relevance to each other, there must be some underlying reason. The truncation procedure, i.e., the

* This work was supported by The National Science Foundation. This paper is based in part on a thesis presented to the University of Connecticut in partial fulfillment of the requirements for the Ph.D. degree.
† Present address: National Bureau of Standards, Washington, D. C.
[1] R. P. Madden and K. Codling, Phys. Rev. Letters **10**, 516 (1963); Astrophys. J. **141**, 364 (1965).
[2] J. A. Simpson, S. R. Mielczarek, and J. W. Cooper, J. Opt. Soc. Am. **54**, 269 (1963).
[3] M. E. Rudd, Phys. Rev. Letters **13**, 503 (1964); H. W. Berry, Phys. Rev. **127**, 1634 (1962).
[4] For example, W. Lichten, Phys. Rev. **131**, 229 (1963).

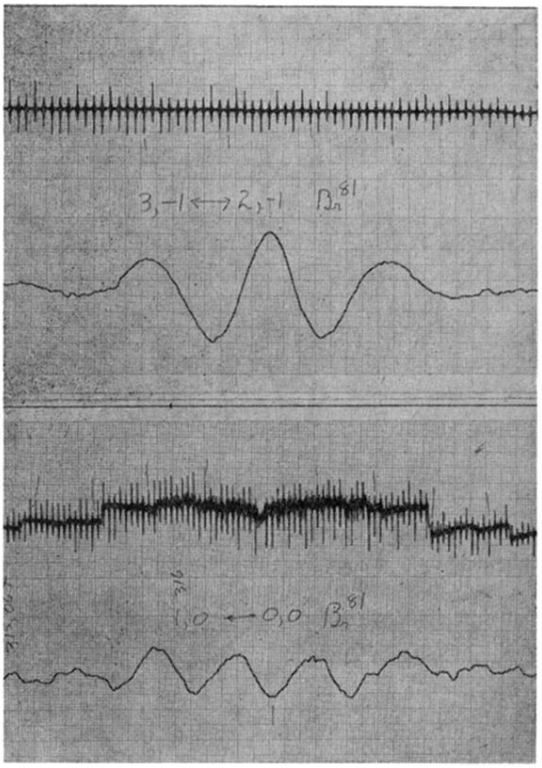

FIG. 5. Representative resonance levels. Top: $(3, -1 \leftrightarrow 2, -1)$ in Br^{81}. Bottom: $(1, 0 \leftrightarrow 0, 0)$ in Br^{81}. Upper trace is frequency indexer $-60\sim$between large spikes.

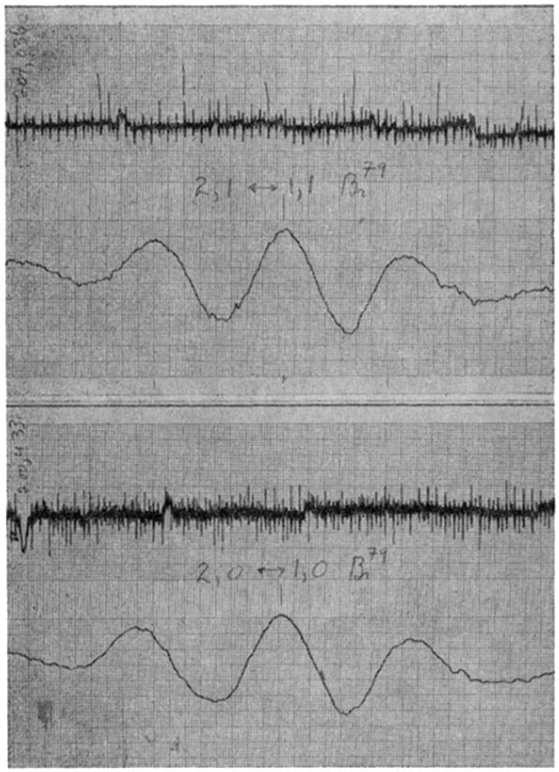

FIG. 6. Representative resonance curves. Top: $(2, 1 \leftrightarrow 1, 1)$ in Br^{79}. Bottom: $(2, 0 \leftrightarrow 1, 0)$ in Br^{79}.